https://doi.org/10.3311/PPme.42845

Periodica Polytechnica Mechanical Engineering

Simulation-based Evaluation of a Schedule-oriented Control Concept for Dual-axis PV Systems in Hungary

Henrik Zsiborács[1*], László Makida[1], András Vincze[1], Nóra Hegedűsné Baranyai[1]

[1] Renewable Energy Research Group, University Center for Circular Economy, University of Pannonia, 18 Zrínyi Miklós street, H-8800 Nagykanizsa, Hungary
[*] Corresponding author, e-mail: zsiboracs.henrik@pen.uni-pannon.hu

Received: 17 November 2025, Accepted: 27 December 2025, Published online: 19 January 2026

Abstract

As a result of the rapid expansion of photovoltaic (PV) systems in Europe, system operators are faced with challenges caused by deviations between scheduled and actual power generation more and more often, which increases their balancing requirements and operational costs. Ensuring schedule compliance has thus become a critical issue for integrating PV into modern electricity networks. This study introduces and evaluates a novel schedule-oriented control mechanism for dual-axis PV systems, based on a patented concept. Unlike conventional sun-tracking strategies that maximize irradiance capture, the proposed method intentionally adjusts module orientation to minimize deviations from day-ahead and intraday schedules. This represents an innovative shift from generation-maximizing to grid-supportive control, directly addressing system-level balancing needs. The control logic, implemented in Python, was evaluated on Hungarian datasets combining measured and simulated time series, and all analyses were carried out in a simulation environment, with field validation planned in future work. Results show that while the mechanism reduces annual energy yield by around 7% (1164 MWh to 1080 MWh per 1 MWp system), it achieves a >90% reduction in downward regulation requirements (from 8.0% to 0.8% of annual output). Upward regulation requirements decreased only marginally, as these cannot be effectively influenced by control interventions. The results demonstrate that the proposed control mechanism substantially improves schedule compliance while incurring only minor energy yield losses, offering a cost-effective solution for large-scale PV integration.

Keywords

PV power plants, solar tracking, schedule compliance, control strategies, grid integration, renewable energy forecasting

1 Introduction

Within the broader context of the energy transition, intermittent renewable energy sources (wind and solar power) have experienced rapid and sustained growth [1, 2]. Their integration into modern power systems has been facilitated by declining technology costs [3, 4], favorable policy instruments [5, 6], and improvements in forecasting [7, 8] and grid integration capabilities [9–11]. In 2024, wind and solar energy combined accounted for approximately 15% of global electricity generation, reflecting their increasingly central role in the global energy mix [12].

PV systems, in particular, have demonstrated exceptional scalability, modularity, and deployment flexibility, making them one of the most rapidly expanding technologies in the global energy portfolio [13, 14]. By early 2025, the cumulative installed PV capacity worldwide reached approximately 2246 GW [15], reflecting exponential growth driven by technological innovation [16], cost reductions in module manufacturing [17], and supportive policy frameworks such as feed-in tariffs, green certificates, and auctions [18–20].

The European Union (EU) continues to play a leading role in global photovoltaic deployment [21, 22], with installed solar PV capacity rising from 207 GW in 2022 to 272.5 GW in 2023, reaching 338 GW by early 2025 [23]. Based on prevailing policy trajectories and investment trends, the total EU capacity could expand to between 549 GW and 719 GW by 2028 [24], depending on the effectiveness of regulatory implementation and the pace of market development [25, 26].

This trend underscores the growing dominance of large-scale solar power plants in Europe's solar energy landscape, particularly in the context of national grid integration and energy market participation. These installations are subject to comprehensive regulatory requirements,

Cite this article as: Zsiborács, H., Makida, L., Vincze, A., Hegedűsné Baranyai, N. "Simulation-based Evaluation of a Schedule-oriented Control Concept for Dual-axis PV Systems in Hungary", Periodica Polytechnica Mechanical Engineering, 2026. https://doi.org/10.3311/PPme.42845

including the submission of day-ahead and intraday generation schedules, compliance with real-time dispatch signals, and participation in balancing markets [27]. In countries with rising solar penetration, these frameworks aim to preserve grid stability while integrating variable renewable generation [28–30].

The reliable and efficient operation of PV power plants is governed by a complex interplay of technological design, environmental conditions, and real-time control strategies. System performance is fundamentally influenced by the type, material composition, and efficiency class of the installed PV modules, as well as their degradation characteristics over time. Additionally, critical site-specific factors – including geographic location, panel orientation (azimuth), tilt angle, degree of surface soiling, and dynamic meteorological conditions such as irradiance, temperature, and cloud cover – have a significant impact on energy yield.

In fixed-tilt PV installations, energy output can be substantially enhanced by optimizing the angle of inclination and orientation according to local solar geometry. Suboptimal alignment or neglecting shading impacts may reduce overall irradiance capture and negatively affect the plant's capacity factor. These losses not only compromise generation efficiency but also prolong the investment payback period and reduce long-term return on investment [31–34]. To mitigate such risks and ensure data-driven performance management, the integration of advanced monitoring systems has become a standard component in modern PV plant infrastructure [35, 36]. These platforms allow operators to remotely track key performance indicators, detect anomalies, and adjust control logic based on real-time measurements [37, 38]. Monitoring systems typically interface with the inverters *via* embedded communication ports or external data acquisition units, and are connected to the Internet through wired (Ethernet) or wireless (Wi-Fi, GSM, LTE) technologies. Most inverter manufacturers offer built-in web servers or standardized communication protocols (e.g., Modbus TCP/IP, MQTT), enabling seamless remote access for authorized personnel [39–41]. Beyond basic fault detection and data logging, advanced monitoring frameworks are increasingly being used to support higher-level functionalities, such as grid-supportive control or predictive maintenance. As PV deployment scales, especially in utility-scale applications, the role of intelligent, responsive monitoring systems becomes ever more crucial – not only for maximizing yield but also for enhancing grid compliance, economic performance, and operational resilience [42, 43].

Although PV power plants play an ever-increasing role in today's electric energy systems [44], their regulation poses a challenge to the optimal management of electricity systems [45, 46].

In order to understand the regulation needs caused by PV power plants and their scale, it is essential to understand the importance of scheduling. Power plants operating in the EU that generate electricity for sale are required to inform the transmission system operator (TSO) of the expected energy generation in a schedule, typically submitted by 12:00 a.m. the day before. The temporal resolution of this is 15 or 60 min in the EU, with the stricter version of 15 min used in Hungary. The task of the TSO is to operate the electricity network efficiently and safely and to transmit electric energy in the high-voltage electricity network in order to ensure the continuity and security of power supply. The scheduling obligation requires power plants to generate electricity at the predetermined times and in the predetermined quantity and feed it into the grid. This obligation is essential to ensure the reliability and balance of electricity supply. In the event of inaccuracies in scheduling, market participants in the EU are obliged to reimburse the costs of imbalances in the energy system caused by their activities.

In the course of schedule keeping there may be a demand for both up- and downward regulation. If the actual power output of a PV power plant falls short of the forecasted value submitted in the schedule, an upward regulation requirement arises to compensate for the energy deficit. Conversely, when the actual production exceeds the scheduled forecast, a downward regulation becomes necessary to prevent grid imbalances. In both cases, the resulting deviations are subject to financial settlement in the balancing energy market, typically coordinated and enforced by the Transmission System Operator (TSO) [47].

An earlier study related to this issue, Zsiborács et al. [48], examined the upward and downward regulation needs of 19 European countries. The research concluded that the accuracy of PV power plant scheduling varied from country to country. It was found that the schedules of PV power plants in Germany and Spain proved to be more accurate than those of other countries. In addition, the research revealed that forecasts in some countries, such as Estonia and Switzerland, showed greater inaccuracies. Hungary, due to strict regulations, has a relatively accurate PV forecasting mechanism in the field of scheduling. The results of the study primarily help energy market participants and decision-makers understand the limitations of the accuracy of forecasting methods. In addition, this

information could contribute to improving the economic efficiency of companies investing in PV power plants through the use of energy storage and other technologies such as solar tracking solutions.

To enhance schedule accuracy and compliance in PV power plants, researchers and system developers are increasingly exploring innovative control strategies. Among these, solar tracking technology has emerged as a promising solution, offering a cost-effective approach to mitigating both upward and downward regulation needs. This paper contributes to this field by introducing a patented control concept (Patent ID: P2300095 [49]) designed to optimize schedule adherence in PV systems equipped with solar tracking capabilities.

The control methodology presented in this paper was formulated as a logical response to Hungary's regulatory environment for PV power plants, particularly with respect to schedule compliance and curtailment capabilities. According to the July 2022 regulations issued by the Hungarian TSO MAVIR (Hungarian Independent Transmission Operator Company Ltd.), all newly installed variable renewable energy units with a nominal capacity above 50 kVA were required to provide a minimum of 30% upward and downward regulation capability (automatic Frequency Restoration Reserve (aFRR)), relative to their installed capacity. This requirement aimed to address rising system balancing costs caused by the increasing share of intermittent solar generation.

However, due to implementation challenges and market feedback, this obligation was temporarily suspended on December 16, 2022. Since then, policy discussions have continued, and according to reports from early 2025, significant regulatory changes may be underway. Notably, a new legislative proposal aims to raise the capacity threshold for mandatory aFRR compliance to 5 MW. If enacted, this change would relieve a substantial number of small- and medium-scale PV plants from the need to install remote-control and regulation capabilities, effectively removing a significant burden from project developers and operators. Nevertheless, the debate remains active. Independent aggregators have expressed concern that such a change might reduce the volume of controllable capacity available to the TSO, potentially undermining grid stability and system flexibility. They advocate for setting the threshold at a more moderate level, such as 400 kW, which would still exempt the smallest systems but preserve the regulatory function of larger non-household PV installations. While the future of mandatory aFRR obligations in Hungary remains uncertain, it is clear that regulatory volatility poses challenges to long-term investment security and system planning. Still, the ongoing evolution of the framework underlines the importance of adaptable technologies and control architectures.

The control concept presented in this paper, supported by a patent (ID: P2300095 [49]), is designed with flexibility and scalability in mind. It addresses the need for cost-effective schedule adherence in PV systems equipped with solar tracking technology. Importantly, it also supports optional integration into aFRR-based grid services, should future regulations reintroduce or redefine such obligations. Given the continuing growth in solar PV capacity, the ability to curtail overproduction and assist in grid balancing remains a valuable capability. Even if formal aFRR compliance becomes optional for a broad segment of the market, being technically prepared for such services offers strategic advantages in terms of both risk mitigation and future revenue potential [50–53].

In order to maximize the annual amount of energy that PV systems can produce, it is essential to know the climatic and territorial conditions of a given site, as this information determines the ideal angle of inclination [54, 55], which varies between 20° and 50° in Europe [56]. To increase the efficiency of PV systems, solar tracking is becoming more and more widespread. Single and dual axis solar tracking systems continuously rotate PV modules towards the sun, resulting in an increase in energy production of up to 20–50% compared to fixed installations. Single-axis solutions are typically east-west, while the dual axis solutions can accurately track the position of the Sun [57–59]. As of 2024, approximately 15–25% of newly installed photovoltaic (PV) power plants employed solar tracking technology. North America was the largest market, accounting for 30% of the global share, while Europe was emerging as the fastest-growing region. The global solar tracker market was valued at around USD 7.01 billion in 2024 and is projected to grow to nearly USD 71.81 billion by 2034, reflecting a compound annual growth rate (CAGR) of 26.2% [60].

Solar tracking photovoltaic (PV) systems can be broadly categorized into active and passive technologies [61–63]. Active tracking systems rely on electromechanical actuators that adjust the orientation of PV modules based on sun position data or sensor inputs. In contrast, passive tracking systems utilize thermomechanical mechanisms, typically involving a compressed fluid with a low boiling point, to facilitate movement in response to solar heating [62, 64].

Currently, active solar tracking systems dominate the market, primarily due to their superior real-time accuracy and adaptability under varying environmental condi-

tions [65]. Among solar tracking methodologies, sensor-based control systems are the most commonly implemented. These systems rely on physical principles, such as differential irradiance detection, to maintain the continuous alignment of PV modules with the brightest point in the sky. However, recent advancements have introduced astronomical equation-based and GPS-assisted tracking systems, which provide a deterministic mechanism for sun positioning without relying on real-time solar irradiance measurements. These approaches are particularly advantageous in regions characterized by frequent cloud coverage or high levels of diffuse radiation, where traditional sensor-based trackers may become unreliable [66]. Although AI-assisted control strategies for solar tracking have demonstrated considerable promise in simulation-based studies and pilot-scale implementations (especially in terms of optimizing energy yield and operational flexibility), their widespread commercial adoption remains constrained. The key limiting factors include high system integration complexity, significant computational requirements, limited field validation, and the absence of standardized deployment frameworks [67].

Despite significant advances in the precision of solar tracking technologies, current control solutions are generally not designed to support grid-aligned generation scheduling. Most existing systems prioritize the maximization of solar irradiance capture and energy yield, but lack mechanisms for dynamic power modulation in accordance with day-ahead or intraday dispatch signals issued by system operators. Recent studies confirm that predictive or schedule-aware control remains largely absent from commercially available and patented tracking systems, which are primarily optimized for real-time solar alignment rather than temporal coordination with grid demands [68, 69].

The following section presents a targeted review of representative commercial products and patented solar tracking control solutions. This analysis evaluates each system's ability – or lack thereof – to integrate schedule-adaptive functionality, thereby contextualizing the relevance and novelty of the control concept proposed in this study (Table 1 [70–80]).

FUSIONSEEKER (Slovenia) has developed a sun tracking control system designed for continuous solar alignment throughout the day [70]. The system disables motor activity during cloudy conditions to conserve energy. Its core functionality is centered on real-time irradiance tracking, and it does not support any mechanisms for aligning generation with grid-based scheduling requirements.

Table 1 Summary overview of reviewed solar tracking control methodologies

System / Patent	Main function	Schedule-adaptive
FUSIONSEEKER [70]	Continuous tracking	No
Solar Stalker (Laser Precision Crafts, LLC) [71]	Configurable delayed tracking	No
EP2389547A4 [72]	Sensor+GPS tracking with wind protection	No
WO2009048879A3 [73]	Performance-based tracking (sensorless)	No
US9291696B2 [74]	Performance-maximizing tracking	No
US20170187327A1 [75]	Optimized motor control (single/dual axis)	No
US20190072992A1 [76]	Forecasting via camera system	No
US10554170B2 [77]	Irradiance/cloud-based forecasting	No
JP2014236541A [78]	Battery charge/discharge control	No
US10139847B2 [79]	PV + battery output stabilization	No
EP3026774B1 [80]	Battery control with grid code	No
Scheduling–Aware*	Schedule-adaptive tracking	Yes

* Note: The Scheduling–Aware control strategy is proposed in the present study.

The Solar Stalker, developed by Laser Precision Crafts, LLC (USA) [71], offers both continuous and delayed sun-tracking modes, with user-configurable delays ranging from 0 to 65 min. During overcast periods, it implements a phased tracking strategy, orienting PV modules toward the brightest part of the sky. Despite this adaptive capability, the system does not include features for dispatch coordination or schedule-aware generation control.

Besides the advanced sun-tracking controllers discussed above, there are also low-cost, mass-produced dual-axis solar tracking units commercially available in 2025 (e.g., [81, 82]), which offer only basic functionality. These systems perform autonomous full-day solar tracking from sunrise to sunset based on optical sensors but lack any form of output modulation, schedule-aware generation, or grid-dispatch coordination. Their design focuses on simple mechanical sun alignment rather than integrated energy management.

The first patent analyzed here, patent EP2389547A4 [72] describes a system that combines sensor data and GPS input to continuously track the sun's trajectory. During

cloud cover, the system relies on GPS-based positioning to continue movement. It also incorporates wind protection features, adjusting panel orientation dynamically in strong gusts. While technically robust, the design remains focused on irradiance optimization and does not support schedule-aligned power output control.

Patent WO2009048879A3 [73] proposes a sensorless system that monitors PV module performance data using an energy collector module to adjust the tracking structure. The solution performs continuous tracking from sunrise to sunset, with the primary objective of maximizing output performance. However, it lacks the ability to modulate generation in coordination with dispatch signals or scheduling plans.

Patent US9291696B2 [74] is similarly centered on maximizing PV output through continuous sun tracking. The control logic does not support any schedule-based modulation or response to grid-oriented requirements, making it unsuitable for dispatch integration.

Patent US20170187327A1 [75] offers greater mechanical flexibility, allowing optimized motor control for both single- and dual-axis systems. The control strategy incorporates solar position, PV output, and wind speed to guide movement. However, this solution remains reactive to environmental conditions only and does not interface with grid dispatch signals or scheduling protocols.

Patent US20190072992A1 [76] focuses on performance forecasting, using a camera-based system to detect environmental conditions and predict PV generation. While valuable for operational planning, this technology does not control solar tracking or manage real-time output and therefore cannot support schedule optimization.

Patent US10554170B2 [77] employs solar irradiance and cloud sensors to anticipate generation fluctuations and evaluate their impact on microgrids and the broader electrical system. Similar to the previous patent, it is designed for performance estimation rather than active tracking control and lacks any scheduling-responsive functionality.

Patent JP2014236541A [78] outlines a real-time battery charging and discharging method linked to PV systems. The approach aims to enhance energy dispatch flexibility *via* storage management. However, it does not alter solar tracking behavior or allow schedule-aligned generation control at the PV level.

Patent US10139847B2 [79] also integrates battery energy storage with PV systems to reduce grid load through optimized production and storage control. Despite this, the control strategy is based solely on real-time system feedback and lacks predictive or schedule-oriented features.

Patent EP3026774B1 [80] introduces a grid code–compliant control solution for PV-battery systems. The core objective is to stabilize battery state-of-charge levels by responding to current network demands. This method remains reactive and does not incorporate any forecasting or schedule-aligned operation at the tracking level.

In summary, the reviewed systems collectively reflect a clear emphasis on real-time sun tracking, environmental adaptability, and in some cases, integration with storage or forecasting components. However, none of the technologies analyzed include a control strategy that actively aligns solar tracking behavior with externally imposed generation schedules. This underscores the relevance of developing a novel control framework that enables photovoltaic systems to meet grid demands not only through maximal energy capture but also through predictive, schedule-adaptive active intervention.

2 Materials and methods

2.1 Empirical basis for simulation inputs: findings from tracking precision analysis

Zsiborács et al. [83] conducted under real meteorological conditions in Hungary evaluated the sensitivity of different PV technologies – monocrystalline (m-Si), polycrystalline (p-Si), and amorphous silicon (a-Si) – to misalignment from the ideal solar tracking position. Using a high-precision dual-axis tracking system equipped with a concentrator photovoltaic (CPV) module as a reference, the study systematically analyzed how deviations from the optimal focus point (FP) affected the electrical performance of each PV type. The experimental protocol involved controlled angular displacements in both tilt and azimuthal directions, with module orientation altered across cardinal and intercardinal directions (N, NW, W, SW, S, SE, E, NE).

The main objective was to determine the so-called performance insensitivity threshold, defined as the angular deviation range in which the PV output remains functionally unaffected. Results showed that for all three PV technologies, performance losses were negligible within a 3° tracking error, regardless of direction. However, beyond this threshold, the angular sensitivity became both technology- and direction-dependent. Deviations in NW, SW, SE, and NE orientations were found to induce the highest performance losses. While all technologies exhibited similar resilience up to moderate misalignments, the performance degradation of amorphous silicon modules became more pronounced above 20°, indicating a higher

directional sensitivity compared to crystalline counterparts under greater angular deviations.

Building on these findings, the present study focuses exclusively on m-Si technology, which dominates newly installed photovoltaic systems across the European Union due to its high efficiency, durability, and favorable cost-performance ratio [84].

To represent the relationship between angular misalignment and performance degradation, the study applied third-degree polynomial regression functions to the measured m-Si data (Table 1 [70–80]), with separate coefficients derived for each of the eight cardinal and intercardinal orientations (N, NW, W, SW, S, SE, E, NE). The polynomial form allows for smooth, continuous approximation of performance changes up to 30° of deviation from the optimal solar vector. The 30° angular limit was maintained in the current simulation model partly due to the limitations of the original measurement dataset, and partly because ±30° represents a typical actuation range for certain types of commercially available linear actuators used in dual-axis solar tracking systems. These polynomial expressions serve as parametric inputs to the control simulation, forming the empirical foundation for evaluating schedule-based strategies.

While studies such as Nsengiyumva et al. [85] report minimal efficiency loss (e.g., <1.5%) at up to 10° of tracking error, the previously reported measurements indicate a more nuanced, direction- and technology-specific degradation pattern – particularly beyond 10°, and markedly so above 20°.

Accordingly, the simulation framework remains grounded in locally measured performance curves, ensuring consistency with Hungary's climatic and radiative conditions. The performance loss of m-Si modules was therefore estimated using the following polynomial expression Eq. (1):

$$f(x) = a + b \times x + c \times x^2 + d \times x^3, \quad (1)$$

where:

- $f(x)$: estimated relative performance (%) at an angular deviation x (°) from the focus point (FP);
- a, b, c, d: direction-specific polynomial regression coefficients obtained from third-degree fits to the measured relative performance data;
- x: angular deviation (in degrees) from the optimal FP.

Table 2 summarizes the regression coefficients corresponding to each cardinal and intercardinal orientation, obtained from third-degree polynomial fits to measured performance loss data as a function of angular deviation from the FP.

Table 2 Polynomial regression coefficients for estimating relative performance of m-Si PV modules as a function of angular deviation from the focus point (FP), by direction. (The regression model is $f(x) = a + bx + cx^2 + dx^3$, where $f(x)$ is the estimated relative performance (%) and is the angular deviation (°) from the FP.)*

Direction	a (baseline value for direction-specific fit)	b (x)	c (x^2)	d (x^3)
North	99.9888	0.0504	−0.0145	0.0001
North-West	100.5779	−0.4611	0.0096	−0.0008
West	100.1443	−0.0665	−0.0167	0.0001
South-West	100.0593	−0.0487	−0.0319	0.0002
South	99.9888	0.0504	−0.0145	0.0001
South-East	99.9491	−0.0052	−0.03	0.0003
East	100.338	−0.225	0.0071	−0.0005
North-East	100.2894	−0.2327	−0.0057	−0.0003

* Note: a, b, c and d are direction-specific polynomial regression coefficients obtained from third-degree fits to the measured relative performance data.

2.2 Control logic design for schedule-adaptive sun-tracking PV systems

Most solar tracking systems currently in operation are active, employing electromechanical actuators controlled by sensor- or algorithm-based strategies. However, the primary limitation of existing systems lies in their exclusive focus on maximizing irradiance capture, without mechanisms for schedule-oriented control or dynamic output adjustment [86].

The conceptual logic of the control strategy presented in this section was designed to improve schedule adherence in sun-tracking PV systems. The new approach is grounded in the growing importance of schedule-keeping capabilities in grid-integrated renewable energy systems, particularly under regulatory frameworks requiring active power control.

To address deviations between forecasted and actual generation, the proposed method introduces a closed-loop control cycle capable of dynamically adjusting the module orientation. This control loop continuously minimizes schedule deviations by adapting the sun-tracking trajectory within predefined tolerance limits.

The control logic is structured as a cyclic procedure, operating at a fixed temporal resolution (e.g., 1-min intervals), and is designed to be integrated into SCADA or EMS-based supervisory architectures.

Fig. 1 illustrates the control flowchart, based on which the complete sequence of operations (S1–S12) can be described in detail. The process begins with S1 – initial-

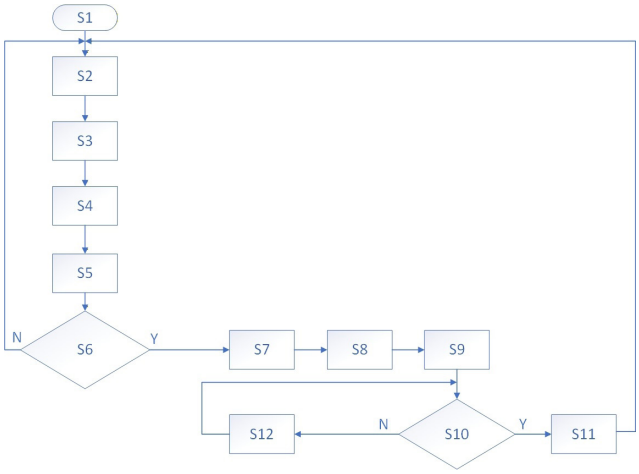

Fig. 1 Schedule-oriented control logic with periodic performance correction for dual-axis solar tracking PV plants

ization, where the control cycle is automatically started and repeated at fixed temporal intervals (e.g., 1-min). In S2 – loading of monitoring data, the system retrieves the day-ahead and intraday schedules submitted to the Transmission System Operator (TSO), as well as the actual generation values recorded by the monitoring system (e.g., SCADA or EMS). Next, S3 – acquisition of the current tracker position provides the actual azimuth and elevation of the PV modules, followed in S4 – solar position computation by the determination of the Sun's real-time position using an integrated algorithm (e.g., SPA), which establishes the reference for orientation and intervention angle calculation. In S5 – quantification of power deviation, the difference between planned and actual generation is calculated in both absolute and percentage form, which is then assessed in S6 – threshold check against a predefined tolerance (e.g., 3%) to avoid unnecessary interventions caused by natural PV fluctuations. If the threshold is exceeded, the process moves to S7 – suspension of default tracking and preparation for intervention, switching from standard dual-axis tracking to schedule-oriented control. This enables S8 – deflection angle determination, where the required adjustment is computed considering the current solar position, actual module orientation, and mechanical limits, ensuring controlled irradiance reduction based on pre-recorded module characteristics. The corresponding commands are executed in S9 – generation of intervention signals, adjusting the azimuth and/or tilt of the PV modules. In S10 – re-evaluation of deviation, the system checks at the next interval whether the deviation has returned within tolerance or whether mechanical limits have been reached. If so, in S11 – sun tracking restart command, once the deviation decreases and the deflection angle compared to the optimal sun position is within 3° the cycle is restarted. Finally, S12 – position stabilization temporarily freezes the orientation (e.g., for 1 min) to avoid excessive actuator movement, after which the cycle restarts from S2.

As part of the post-processing analysis, the simulation results were examined to quantify how often the system experienced two characteristic conditions: persistent underperformance (when the corrected output remained below the schedule) and mechanical limit events (when the actuator reached its mechanical deflection limit and no further adjustment was possible).

For each control interval, the relationship between corrected and scheduled generation was assessed, classifying each step as underperformance when the corrected output was lower than the scheduled value, and as mechanical bound when it exceeded the scheduled value despite active regulation.

The occurrence frequencies were then computed as the ratio of these cases to the total number of control steps, expressed as a percentage.

The practical implementation of this control sequence, along with its mathematical formalization, is presented in the Results section. The proposed logic was fully developed and executed in a Python-based environment (3.12.5) [87].

2.3 Data sources and preprocessing

The first dataset was obtained from the ENTSO-E Transparency Platform (Platform), a public database operated by European transmission system operators. It contains day-ahead, intraday, and actual generation data for renewable sources, reported in 15-min resolution and harmonized across EU member states. For this study, datasets were retrieved for Hungary's entire portfolio of PV power plants subject to scheduling obligations, covering the full year 2024. These data served to quantify deviations between forecasted and actual generation for fixed-tilt PV systems. All values were normalized to a nominal capacity of 1 MWp.

The second dataset was generated using the HOMER Pro simulation software (3.18.4) [88], a widely applied energy system modeling tool used in the analysis and optimization of renewable-based systems. Based on the geographical coordinates and climatic conditions of the study site (Keszthely, Hungary), the HOMER Pro simulation software (3.18.4) [88] produced generation time series for a dual-axis tracking PV plant with a nominal capacity of 1 MW. This location corresponds to the site referenced in Section 2.1 [83], and the previously derived polynomial

regression functions were used as parametric inputs for simulating schedule-based control strategies.

The data-preparation workflow consisted of five sequential steps:

1. interpolation of the simulated HOMER Pro dataset [88] to 15-min resolution,
2. ratio-based correction against measured ENTSO-E data with median replacement for outliers,
3. synchronization of the corrected series with schedule data,
4. derivation and capping of the dual-axis schedule (maximum 960 kW), and
5. consistency check for zero-schedule intervals.

These steps ensured full alignment between simulated and measured datasets and provided robust inputs for schedule-based control evaluation. To ensure compatibility between the two data sources, a series of preprocessing steps was required, as detailed below:

1. Temporal resolution harmonization: the HOMER Pro simulation software [88] provided hourly time series $\left(P_t^{\text{HOMER}}\right)$. These data were linearly interpolated to a 15-min resolution in order to be directly comparable with the schedule $\left(M_t^{\text{fix}}\right)$ and actual generation $\left(P_t^{\text{Platform}}\right)$ datasets obtained from the Platform, which are also reported at 15-min intervals. During interpolation, each hourly value was complemented with two intermediate points, ensuring a continuous time series.
2. Reference-based correction of simulated data: since the Platform datasets $\left(P_t^{\text{Platform}}\right)$ represent actual power generation, they were considered as reference values. Accordingly, the HOMER Pro simulated series $\left(P_t^{\text{HOMER}}\right)$ were corrected by calculating, for each 15-min interval, the ratio between the simulated and the actual Platform values, expressed as:

$$R_t = \frac{P_t^{\text{HOMER}}}{P_t^{\text{Platform}}}, \tag{2}$$

where:

- R_t: ratio in a given time interval t,
- P_t^{HOMER}: simulated actual power from HOMER Pro [88] (MW),
- P_t^{Platform}: actual power from the Platform (fixed system) (MW).

This ratio (R_t) expressed the magnitude of deviation between the simulated values $\left(P_t^{\text{HOMER}}\right)$ and the actual values $\left(P_t^{\text{Platform}}\right)$. The obtained ratios were subsequently grouped by time-of-day segments, and for each segment a representative "typical" value was determined, using the median as a robust estimator. Outliers were defined as those ratios that exceeded five times, or fell below one-fifth, of the median value for the corresponding time segment. The application of this threshold served as a statistical filter for extreme deviations, ensuring that the overall profile of the time series remained realistic. Ratios exceeding these thresholds typically originated from the limitations of the simulation model (HOMER Pro [88]), which, for example, tended to overestimate power generation during morning ramp-up and evening decline periods compared to the actual Platform measurements. Such extreme values were replaced with the median of the respective time segment, thereby mitigating distortions and eliminating unrealistic fluctuations from the dataset.

The corrected HOMER Pro [88] time series $\left(P_t^{\text{HOMER},corr}\right)$ was generated by multiplying the software-simulated performance values $\left(P_t^{\text{HOMER}}\right)$ with the cleaned and representative ratio ($f(R_t)$), as defined by the following equation (Eq. (3)):

$$P_t^{\text{HOMER},corr} = P_t^{\text{HOMER}} \times f\left(R_t\right), \tag{3}$$

where:

- $P_t^{\text{HOMER},corr}$: corrected HOMER Pro [88] simulated actual performance at time t (MW),
- $f(R_t)$: time-of-day–specific cleaned and representative ratio.

This ensured that the corrected dataset preserved the general characteristics of the actual system output while representing a dual-axis configuration.

3. Synchronization with schedule data: After the synchronization of the corrected HOMER Pro dataset [88] $\left(P_t^{\text{HOMER},corr}\right)$ with the fixed system schedule data provided by the Platform $\left(M_t^{\text{fix}}\right)$ only those 15-min intervals were retained for which valid schedule values existed. Time periods without scheduled values (e.g., early morning hours when actual production was zero) were excluded.
4. Estimation of schedule data for the dual-axis system: The Platform provides schedule data exclusively for fixed-tilt systems $\left(M_t^{\text{fix}}\right)$, which are always linked to their corresponding actual performance time series $\left(P_t^{\text{fix}}\right)$. Since no paired schedule dataset was available for the dual-axis system, its schedule had to be derived from the fixed-tilt system schedules. For this purpose, in each 15-min interval the ratio between the corrected HOMER Pro [88] dual-axis actual performance $\left(P_t^{dual,corr}\right)$ and the Platform-based fixed

actual performance $\left(P_t^{\text{fix}}\right)$ was calculated. This ratio is hereinafter denoted as $\left(R_t^{dual}\right)$. This ratio $\left(R_t^{dual}\right)$ indicates the relative difference in generation between the dual-axis and the fixed-tilt systems at a given time, showing whether the dual-axis configuration would have produced a surplus or deficit compared to the fixed system. Accordingly, the dual-axis schedule $\left(M_t^{dual}\right)$ was estimated as follows:

$$M_t^{dual} = M_t^{\text{fix}} \times \frac{P_t^{dual,corr}}{P_t^{\text{fix}}}, \tag{4}$$

$$M_t^{dual} = M_t^{\text{fix}} \times R_t^{dual}, \tag{5}$$

where:

- M_t^{dual} : estimated schedule for the dual-axis system at time t (MW),
- M_t^{fix} : schedule for the fixed-tilt system (Platform) (MW),
- $P_t^{dual,corr}$: corrected HOMER Pro [88] dual-axis actual performance (MW),
- P_t^{fix} : actual performance of the fixed-tilt system (Platform) (MW),
- R_t^{dual} : ratio between dual-axis and fixed-tilt actual performance at time t (MW).

Extreme ratios were replaced with typical values determined on a time-of-day basis, and an upper cap of 960 kW was applied, corresponding to the typical maximum output of a nominal 1 MW PV system.

5. Consistency check: In time intervals where the estimated dual-axis schedule $\left(M_t^{dual}\right)$ equaled zero, the corresponding corrected actual performance $\left(P_t^{dual,corr}\right)$ was also set to zero. This ensured that no situations occurred where the schedule indicated zero output while the actual data showed positive generation. This step further improved the consistency and robustness of the dataset.

To confirm the robustness of these preprocessing settings, a brief sensitivity check was performed regarding the interpolation scheme, the median-based outlier replacement, and the applied capping threshold. This verification indicated that the methodological choices had only marginal influence on the overall outcomes.

2.4 Methodology for assessing schedule accuracy and regulation requirements

In this study, the methodology presented in Zsiborács et al. [27] was adopted to evaluate schedule-keeping accuracy and to quantify up- and down-regulation requirements. The aim of the analysis is to demonstrate how the mechanism developed in the present research can mitigate schedule deviations and thereby reduce regulation needs.

Throughout this section, M_t denotes the scheduled generation, $P_t^{dual,corr}$ the corrected actual generation, and $P_t^{dual,mech}$ the mechanism-adjusted actual generation.

The starting point of the analysis was the corrected dual-axis actual performance dataset $\left(P_t^{dual,corr}\right)$, along with the corresponding schedule values $\left(M_t^{dual}\right)$. For the assessment of schedule keeping accuracy, however, two types of actual performance were considered:

- the corrected simulation-based dual-axis actual data $\left(P_t^{dual,corr}\right)$, and
- the mechanism-adjusted dual-axis actual data introduced in this study $\left(P_t^{dual,mech}\right)$.

The average magnitude of the regulation requirement was quantified using the Mean Absolute Error (MAE) indicator:

$$\text{MAE}^{dual,corr} = \frac{1}{N}\sum_{i=1}^{N}\left|M_{t,i}^{dual} - P_{t,i}^{dual,corr}\right|, \tag{6}$$

$$\text{MAE}^{dual,mech} = \frac{1}{N}\sum_{i=1}^{N}\left|M_{t,i}^{dual} - P_{t,i}^{dual,mech}\right|, \tag{7}$$

where:

- N: number of observed time intervals,
- $P_t^{dual,mech}$: dual-axis actual performance at time t, modified by the mechanism introduced in the present study (MW).

While MAE provides the overall magnitude of deviations, it does not differentiate their direction. Therefore, the breakdown of deviations is necessary, since negative and positive errors are associated with distinct regulatory costs and market implications. Accordingly, two additional indicators were introduced:

- The Mean Negative Error (MNE) was introduced to quantify positive imbalances (actual output > scheduled output), corresponding to down-regulation requirements:

$$\text{MNE}^{dual,corr} = \frac{1}{N}\sum_{i=1}^{N}\min\left(0, M_{t,i}^{dual} - P_{t,i}^{dual,corr}\right), \tag{8}$$

$$\text{MNE}^{dual,mech} = \frac{1}{N}\sum_{i=1}^{N}\min\left(0, M_{t,i}^{dual} - P_{t,i}^{dual,mech}\right). \tag{9}$$

- On the other hand, the Mean Positive Error (MPE) quantifies negative imbalances (actual output < scheduled output), which translate into up-regulation requirements:

$$\mathrm{MPE}^{dual,corr} = \frac{1}{N}\sum_{i=1}^{N}\max\left(0, M_{t,i}^{dual} - P_{t,i}^{dual,corr}\right), \quad (10)$$

$$\mathrm{MPE}^{dual,mech} = \frac{1}{N}\sum_{i=1}^{N}\max\left(0, M_{t,i}^{dual} - P_{t,i}^{dual,mech}\right). \quad (11)$$

The two components together yield the total deviation:

$$\mathrm{MAE} = |\mathrm{MNE}| + \mathrm{MPE}. \quad (12)$$

This methodological framework enables the quantification of both downward and upward regulation requirements for the corrected dual-axis case $\left(M_{t,i}^{dual}, P_{t,i}^{dual,corr}\right)$ as well as for the mechanism-adjusted case $\left(M_{t,i}^{dual}, P_{t,i}^{dual,mech}\right)$. On this basis, it is possible to evaluate to what extent the proposed mechanism can effectively reduce schedule deviations and the associated balancing energy needs.

Furthermore, the total annual actual energy production was also calculated for both cases (i.e., without and with the mechanism) to provide a consistent basis for comparison of schedule deviations in relative terms. The annual energy production was derived as follows:

$$E^{dual,corr} = \sum_{t=1}^{N} P_t^{dual,corr} \times \Delta t, \quad (13)$$

$$E^{dual,mech} = \sum_{t=1}^{N} P_t^{dual,mech} \times \Delta t, \quad (14)$$

where:

- $E^{dual,corr}$: annual actual energy production of the corrected dual-axis system without the mechanism (MWh),
- $E^{dual,mech}$: annual actual energy production of the dual-axis system with the mechanism applied (MWh),
- Δt: time step (0.25 h) (h).

3 Results and discussion

3.1 Implementation and mathematical formalization of the schedule-tracking mechanism

As a result of the present research, the schedule-tracking mechanism developed by the authors is presented below. The decision logic was implemented in Python [87], enabling the automated processing of large time series datasets and the numerical simulation of the operation of the mechanism.

The purpose of the mechanism is to modify the corrected dual-axis actual performance $\left(P_t^{dual,corr}\right)$ in such a way that it follows the scheduled values $\left(M_t^{dual}\right)$ as closely as possible.

The decision-making process can be mathematically formalized through the following rules:

1. Exact schedule adherence:
   If the corrected actual performance equals the scheduled value, no adjustment is required. This case corresponds to perfect alignment, where the actual generation already matches the schedule. Hence, the mechanism remains inactive:
   $$P_t^{dual,mech} = P_t^{dual,corr}, \text{ if } P_t^{dual,corr} = M_t^{dual}. \quad (15)$$
2. Deviation within tolerance band:
   If the deviation remains smaller than a predefined relative threshold (ε), no intervention is performed. This band prevents unnecessary adjustments for small fluctuations that may arise from measurement noise or natural short-term irradiance variability:
   $$P_t^{dual,mech} = P_t^{dual,corr}, \text{ if } \left|\Delta P_t\right| < \varepsilon \times M_t^{dual}, \quad (16)$$
   where:
   - $\Delta P_t = P_t^{dual,corr} - M_t^{dual}$: deviation between actual and scheduled performance,
   - ε: predefined tolerance threshold (dimensionless).
3. Underperformance $\left(P_t^{dual,corr} < M_t^{dual}\right)$:
   The system actively increases the output by reorienting the PV modules toward the optimal solar position. Here the mechanism assumes that the deviation can be compensated by improving the orientation of the modules. The function $f(\theta_t)$ accounts for the irradiance gain achievable through optimal tracking:
   $$P_t^{dual,mech} = f\left(\theta_t\right) \times P_t^{dual,corr}, \text{ if } P_t^{dual,corr} < M_t^{dual}, \quad (17)$$
   where:
   - $f(\theta t)$: power reducing function of the module tilt angle θ_t.
4. Overproduction $\left(P_t^{dual,corr} > M_t^{dual}\right)$:
   The system reduces the output by adjusting the modules' tilt angle away from the optimal solar position This intentional detuning reduces generation to avoid exceeding the scheduled value, ensuring that the plant does not feed more power than planned into the grid:
   $$P_t^{dual,mech} = f\left(\theta_t\right) \times P_t^{dual,corr}, \text{ if } P_t^{dual,corr} > M_t^{dual}. \quad (18)$$
5. Persistent underperformance despite optimal positioning:
   If the scheduled value cannot be achieved even with optimal module orientation, the actual performance remains unchanged:
   $$P_t^{dual,mech} = P_t^{dual,corr}, \text{ if } P_t^{dual,corr} < M_t^{dual} \wedge \text{optimal positioning is insufficient}, \quad (19)$$

where:

- optimal positioning: denotes the case when modules are oriented at the optimal solar position.

This case reflects a physical limitation of the system. Even under full solar tracking, the available irradiance may be insufficient to meet the scheduled output. In such situations, the mechanism cannot further increase production, and defaults to the corrected actual performance $P_t^{dual,corr}$ without additional adjustment.

6. Compact decision rule:
   The above cases can be summarized in the following unified expression:

$$P_t^{dual,mech} = \begin{cases} P_t^{dual,corr} P_t^{dual,corr} M_t^{dual} \\ P_t^{dual,corr} \left|\Delta P_t\right| M_t^{dual} \\ \left(\theta_t\right) \times P_t^{dual,corr} P_t^{dual,corr} M_t^{dual} \\ \left(\theta_t\right) \times P_t^{dual,corr} P_t^{dual,corr} M_t^{dual} \\ P_t^{dual,corr} \end{cases}. \quad (20)$$

   Equation (20) provides a compact mathematical summary of the mechanism. It captures all possible cases of deviation, ranging from exact compliance to physical underperformance limits, and formalizes the corrective logic in a unified framework. This unified formulation also facilitates implementation in algorithmic or simulation environments, enabling its practical application for schedule adherence and regulation studies.

For reproducibility, a simplified pseudocode representation of the control loop is provided in Appendix A, illustrating the Python-based implementation logic and its MicroPython-portable structure (1.23.0) [89].

3.2 The design of the newly developed control procedure

Based on the simulation, the annual actual energy production of the corrected dual-axis system ($E^{dual,corr}$) amounted to 1164 MWh for a nominal installed capacity of 1 MWp. This value was used as the reference for normalizing schedule deviations, thereby enabling the quantification of the relative magnitude of regulation requirements.

In the case of day-ahead forecasts, the downward regulation requirement accounted for 8.0% of the annual energy production. This indicates that during the examined period, the actual production exceeded the scheduled values by this proportion, implying a corresponding need for downward regulation from the system operator. At the same time, the upward regulation requirement reached 7.9%, reflecting periods when the actual production was lower than the scheduled output, thus necessitating upward regulation reserves.

For intraday forecasts, the downward regulation requirement was reduced to 7.0% of the annual energy production. This suggests that short-term forecasts were more accurate, resulting in fewer deviations caused by excess production compared to the schedule. Conversely, the upward regulation requirement remained practically unchanged at 6.9%, showing that production shortfalls persisted even with improved forecast accuracy.

Overall, in the case without the mechanism, the simulated annual production of the dual-axis system ($E^{dual,corr}$) was characterized by both downward and upward regulation requirements in the range of 7–8% of the total energy. These findings are consistent with the results reported in the authors' previous study in Zsiborács et al. [48], which reported similar magnitudes of deviations across PV systems in various ENTSO-E countries (Table 3).

With the application of the mechanism, the corrected annual energy yield of the dual-axis system ($E^{dual,mech}$) amounted to 1080 MWh, which represents approximately a 7% reduction compared to the 1164 MWh obtained without the mechanism ($E^{dual,corr}$). This reduction is a direct consequence of the control logic, which in certain periods deliberately curtailed actual production in order to maintain schedule compliance.

The downward regulation requirement decreased substantially, from 8.0% without the mechanism to 0.8% with the mechanism in place. This represents a relative improvement of more than 90%, clearly demonstrating the effectiveness of the control logic in mitigating schedule deviations caused by overproduction, thereby minimizing the magnitude of downward regulation needs.

In contrast, the upward regulation requirement decreased only marginally, from 6.94% to 6.9%. This negligible improvement indicates that the mechanism is not capable of substantially influencing the regulation demand associated with production shortfalls. This is expected, as the mechanism is primarily designed to reduce excess generation, while shortage situations are inherently constrained by the available solar irradiance, which cannot be increased by control interventions.

Overall, the application of the mechanism resulted in a modest reduction in annual energy yield (approximately 7%) but significantly enhanced schedule adherence. Its effectiveness was most evident in reducing downward regulation requirements, thereby alleviating a major source of balancing demand for the power system (Table 3).

Table 3 Annual corrected simulated energy production and schedule deviations for the dual-axis PV system (1 MWp)

Forecast type	Indicator	Without mechanism (%)	With mechanism (%)	Relative reduction (%)
Day-ahead	MNE_E^{dual} (%)	8.0	0.8	90
	MPE_E^{dual} (%)	7.9	7.8	1
Intraday	MNE_E^{dual} (%)	7.0	0.4	94
	MPE_E^{dual} (%)	6.9	6.9	0

The indicators shown in Table 3 are defined as follows:

- MNE_E^{dual} : Mean Negative Error expressed as a percentage of total annual energy production,
- MPE_E^{dual} : Mean Positive Error expressed as a percentage of total annual energy production.

Fig. 2 presents scatter plots comparing the scheduled values (x-axis) and the actual energy production (y-axis) for the cases without and with the mechanism, under both day-ahead and intraday forecasts. The diagonal line represents the hypothetical case of perfect agreement between schedule and actual values, and deviations can thus be interpreted relative to this line:

- Day-ahead without the mechanism: the scatter cloud shows considerable dispersion around the diagonal. In several cases, the scheduled power output significantly deviated from the actual production, especially at higher generation levels, illustrating the magnitude of downward regulation requirements.

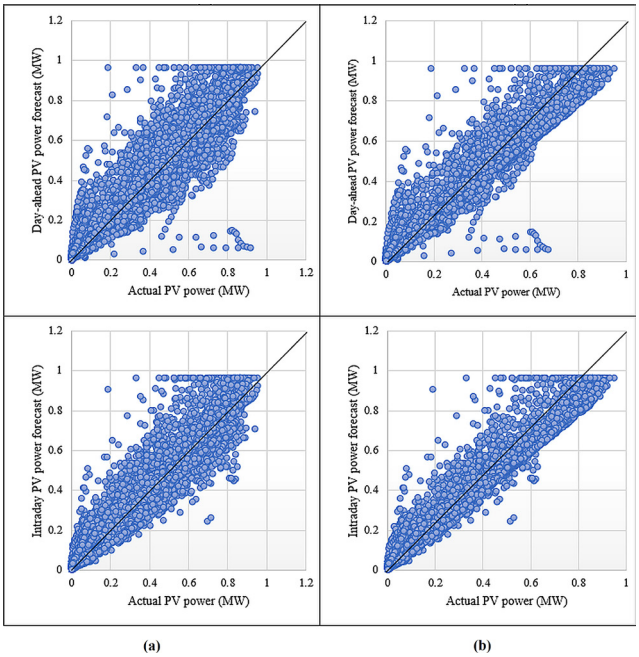

Fig. 2 Scatter plots of day-ahead and intraday forecast versus actual dual-axis PV power, with and without the proposed mechanism (1 MWp reference system): (a) Without mechanism; (b) With mechanism

- Intraday without the mechanism: the scatter cloud is located closer to the diagonal compared to the day-ahead case, reflecting the inherently higher accuracy of intraday forecasts.
- Day-ahead with the mechanism: the scatter points cluster more tightly around the diagonal compared to the case without the mechanism. This indicates, on the one hand, that the mechanism substantially mitigated schedule deviations arising from overproduction, and on the other hand, that the more controlled actual energy production resulted in a distribution more closely aligned with the diagonal.
- Intraday with the mechanism: the scatter points cluster even more tightly around the diagonal than in the day-ahead case with the mechanism, representing the highest level of accuracy among the four scenarios. While perfect alignment cannot be achieved, the distribution of points representing scheduled versus actual values is noticeably narrower compared to the intraday case without the mechanism, and also shows a tighter fit relative to the day-ahead case. This confirms that the mechanism, when combined with intraday forecasts, provides the most effective improvement in schedule adherence.

To quantitatively complement Fig. 2 and substantiate the interpretation of unchanged upward regulation, the frequency of key control outcomes was analyzed.

In the day-ahead forecast case, persistent underperformance at optimal orientation occurred in 27.3% of control intervals, typically under sub-optimal irradiance when available solar input could not meet the scheduled target.

Mechanical limits (S8–S10) were reached in 6.38% of intervals, indicating that physical constraints were encountered during high-irradiance periods where further curtailment was not feasible.

For the intraday forecast case, persistent underperformance occurred in 24.3% of intervals, while mechanical limits were reached in 6.43% of intervals.

The tolerance threshold (ε) applied in both simulations was 3%, below which no corrective action was triggered (S6).

4 Conclusions

This study presented a schedule keeping mechanism based on a patented concept, designed to mitigate balancing energy requirements arising from schedule deviations in dual-axis photovoltaic (PV) systems. According to the results, the proposed solution reduced downward

regulation needs by more than 90%, while annual energy production decreased by only 7%. This demonstrates that PV systems equipped with solar tracking can, beyond optimizing energy production, also provide active flexibility services to the system operator, thereby contributing to power system stability. At the same time, upward regulation requirements remained practically unchanged, indicating that the mechanism is not capable of substantially reducing production shortfalls.

The control logic was initially developed as a decision-making process, which was then implemented in Python to verify its feasibility, confirming the viability of the concept, which was subsequently formalized in the form of a mathematical model. An additional advantage of the Python-based implementation is that several of its modules can be directly transferred to a MicroPython environment, thus enabling prototype-level real-time control implementation. In addition to the preprocessing verification described earlier, minor consistency checks were also carried out to ensure that the model's main performance indicators (MNE, MPE, and downward regulation reduction) remained stable across different parameter configurations and data conditions. No systematic deviations were observed, even during ramp or atypical irradiance periods, which further supports the robustness of the simulation outcomes. The program structure is modular and flexible, allowing its components to be adapted individually and configured according to the specific technical parameters of a given PV plant.

Future research will focus on the practical validation of the model in experimental or pilot systems, where operational experience can further refine the control logic. However, the strict regulatory framework currently in place in Hungary poses significant constraints on the wide-scale practical implementation of schedule keeping trials. Nevertheless, the proposed concept holds considerable potential in reducing scheduling deviations and, in the long term, may contribute to a more efficient system-level integration of solar energy. Further investigations will target the alignment of regulatory frameworks with technological opportunities, with particular emphasis on the integration of energy storage.

Acknowledgement

We acknowledge the financial support of 2021-1.2.6-TÉT-IPARI-MA-2022-00025 financed from the National Research, Development and Innovation Office (NRDI) Fund.

References

[1] Gayen, D., Chatterjee, R., Roy, S. "A review on environmental impacts of renewable energy for sustainable development", International Journal of Environmental Science and Technology, 21(5), pp. 5285–5310, 2024. https://doi.org/10.1007/s13762-023-05380-z

[2] Guchhait, R., Sarkar, B. "Increasing Growth of Renewable Energy: A State of Art", Energies, 16(6), 2665, 2023. https://doi.org/10.3390/en16062665

[3] Bogdanov, D., Ram, M., Aghahosseini, A., Gulagi, A., Oyewo, A. S., …, Breyer, C. "Low-cost renewable electricity as the key driver of the global energy transition towards sustainability", Energy, 227, 120467, 2021. https://doi.org/10.1016/j.energy.2021.120467

[4] Kumar, A., Pal, D. B. "Renewable Energy Development Sources and Technology: Overview", In: Kumar, S., Singh, V. K. (eds.) Renewable Energy Development: Technology, Material and Sustainability, Springer Singapore, 2025, pp. 1–23. ISBN 978-981-97-9626-7 https://doi.org/10.1007/978-981-97-9626-7_1

[5] Mirza, Z. T., Anderson, T., Seadon, J., Brent, A. "A thematic analysis of the factors that influence the development of a renewable energy policy", Renewable Energy Focus, 49, 100562, 2024. https://doi.org/10.1016/j.ref.2024.100562

[6] Bashir, M. F., Sadiq, M., Talbi, B., Shahzad, L., Adnan Bashir, M. "An outlook on the development of renewable energy, policy measures to reshape the current energy mix, and how to achieve sustainable economic growth in the post COVID-19 era", Environmental Science and Pollution Research, 29(29), pp. 43636–43647, 2022. https://doi.org/10.1007/s11356-022-20010-w

[7] Bamisile, O., Oluwasanmi, A., Obiora, S., Osei-Mensah, E., Asoronye, G., Huang, Q. "Application of deep learning for solar irradiance and solar photovoltaic multi-parameter forecast", Energy Sources, Part A: Recovery, Utilization, and Environmental Effects, 46(1), pp. 13237–13257, 2024. https://doi.org/10.1080/15567036.2020.1801903

[8] Qin, J., Jiang, H., Lu, N., Yao, L., Zhou, C. "Enhancing solar PV output forecast by integrating ground and satellite observations with deep learning", Renewable and Sustainable Energy Reviews, 167, 112680, 2022. https://doi.org/10.1016/j.rser.2022.112680

[9] Ejuh Che, E., Roland Abeng, K., Iweh, C. D., Tsekouras, G. J., Fopah-Lele, A. !The Impact of Integrating Variable Renewable Energy Sources into Grid-Connected Power Systems: Challenges, Mitigation Strategies, and Prospects", Energies, 18(3), 689, 2025. https://doi.org/10.3390/EN18030689

[10] Abualoyoun, O. S., Amar, A. A. "Advancing the Global Integration of Solar and Wind Power: Current Status and Challenges", The International Journal of Electrical Engineering and Sustainability (IJEES), 3(2), pp. 73–88, 2025. [online] Available at: https://ijees.org/index.php/ijees/article/view/127 [Accessed: 15 September 2025]

[11] Cao, Y., Xu, B., Zhang, C., Li, F.-F., Liu, Z. "Strategic site-level planning of VRE integration in hydro-wind-solar systems under uncertainty", Energy, 328, 136523, 2025. https://doi.org/10.1016/j.energy.2025.136523

[12] Graham, E., Fulghum, N., Altieri, K. "Global Electricity Review 2025", Ember, London, UK, 2025. [online] Available at: https://ember-climate.org/insights/research/global-electricity-review-2025/ [Accessed: 15 September 2025]

[13] Ahmed, S., Ali, A., Ahmed Ansari, J., Abdul Qadir, S., Kumar, L. "A Comprehensive Review of Solar Photovoltaic Systems: Scope, Technologies, Applications, Progress, Challenges, and Recommendations", IEEE Access, 13, pp. 69723– 69750, 2025. https://doi.org/10.1109/ACCESS.2025.3558539

[14] Massano, M., Domingo, C. M., Macii, E., Patti, E., Bottaccioli, L. "A scalable and flexible solution to evaluate the effects of the integration of photovoltaic distributed generation systems within the electrical grid", Sustainable Energy, Grids and Networks, 43, 101732, 2025. https://doi.org/10.1016/j.segan.2025.101732

[15] Masson, G., Van Rechem, A., de l'Epine, M., Jäger-Waldau, A. "Snapshot of Global PV Markets 2025: Task 1 Strategic PV Analysis and Outreach", [pdf] International Energy Agency Photovoltaic Power Systems Programme (IEA PVPS), 2025. Available at: https://iea-pvps.org/wp-content/uploads/2025/04/Snapshot-of-Global-PV-Markets_2025.pdf [Accessed: 15 September 2025]

[16] Nijsse, F. J. M. M., Mercure, J.-F., Ameli, N., Larosa, F., Kothari, S., Rickman, J., Vercoulen, P., Pollitt, H. "The momentum of the solar energy transition", Nature Communications, 14(1), 6542, 2023. https://doi.org/10.1038/s41467-023-41971-7

[17] Chang, N. L., Newman, B. K., Egan, R. J. "Future cost projections for photovoltaic module manufacturing using a bottom-up cost and uncertainty model", Solar Energy Materials and Solar Cells, 237, 111529, 2022. https://doi.org/10.1016/j.solmat.2021.111529

[18] Lage, M., Castro, R. "A Practical Review of the Public Policies Used to Promote the Implementation of PV Technology in Smart Grids: The Case of Portugal", Energies, 15(10), 3567, 2022. https://doi.org/10.3390/en15103567

[19] Fu, Y., Yang, C., Zhang, L., Wang, L., Jiang, K. "Regional feed-in tariff mechanism for photovoltaic power generation in China considering tradable green certificate revenue", Journal of Cleaner Production, 436, 140641, 2024. https://doi.org/10.1016/j.jclepro.2024.140641

[20] Yu, X., Ge, S., Zhou, D., Wang, Q., Chang, C.-T., Sang, X. "Whether feed-in tariff can be effectively replaced or not? An integrated analysis of renewable portfolio standards and green certificate trading", Energy, 245, 123241, 2022. https://doi.org/10.1016/J.ENERGY.2022.123241

[21] Jäger-Waldau, A., Kakoulaki, G., Taylor, N., Szábo, S. "The Role of the European Green Deal for the Photovoltaic Market Growth in the European Union", In: 2022 IEEE 49th Photovoltaic Specialists Conference (PVSC), Philadelphia, PA, USA, 2022, pp. 0508–0511. ISBN 978-1-7281-6117-4 https://doi.org/10.1109/PVSC48317.2022.9938529

[22] Aleksandra, A., Sara, B. P., Małgorzata, J., Brian, B., Davide, P., Miguel, C. "Role of solar PV in net-zero growth: An analysis of international manufacturers and policies", Progress in Photovoltaics, 32(9), pp. 607–622, 2024. https://doi.org/10.1002/pip.3797

[23] European Commission "Solar energy", [online] Available at: https://energy.ec.europa.eu/topics/renewable-energy/solar-energy_en [Accessed: 14 July 2025]

[24] SolarPower Europe "European Market Outlook for Solar Power 2024-2028", SolarPower Europe, 2024. ISBN 9789464669237 [online] Available at: https://solarpowereurope.eu/ [Accessed: 15 September 2025]

[25] Chatzipanagi, A., Jäger-Waldau, A., Letout, S., Mountraki, A., Bermudez, J. G., Georgakaki, A., Ince, E., Schmitz, A. "Clean Energy Technology Observatory, Photovoltaics in the European Union - Status Report on Technology Development, Trends, Value Chains & Markets: 2024", Publications Office of the European Union, Luxembourg, Luxembourg, Rep. KJ-01-24-077-EN-N, 2024. https://doi.org/10.2760/1812909

[26] Kougias, I., Taylor, N., Kakoulaki, G., Jäger-Waldau, A. "The role of photovoltaics for the European Green Deal and the recovery plan", Renewable and Sustainable Energy Reviews, 144, 111017, 2021. https://doi.org/10.1016/j.rser.2021.111017

[27] Zsiborács, H., Pintér, G., Vincze, A., Baranyai, N. H., Mayer, M. J. "The reliability of photovoltaic power generation scheduling in seventeen European countries", Energy Conversion and Management, 260, 115641, 2022. https://doi.org/10.1016/j.enconman.2022.115641

[28] Fresia, M., Bordo, L., Delfino, F., Bracco, S. "Optimal day-ahead active and reactive power management for microgrids with high penetration of renewables", Energy Conversion and Management: X, 23, 100598, 2024. https://doi.org/10.1016/j.ecmx.2024.100598

[29] Diahovchenko, I., Morva, G., Chuprun, A., Keane, A. "Comparison of voltage rise mitigation strategies for distribution networks with high photovoltaic penetration", Renewable and Sustainable Energy Reviews, 212, 115399, 2025. https://doi.org/10.1016/j.rser.2025.115399

[30] Hossain, M. D. S., Wadi Al-Fatlawi, A., Kumar, L., Fang, Y. R., Assad, M. E. H. "Solar PV high-penetration scenario: an overview of the global PV power status and future growth", Energy Systems, 2024. https://doi.org/10.1007/s12667-024-00692-6

[31] Klugmann-Radziemska, E. "Shading, Dusting and Incorrect Positioning of Photovoltaic Modules as Important Factors in Performance Reduction", Energies, 13(8), 1992, 2020. https://doi.org/10.3390/EN13081992

[32] Tang, L., Liu, Y., Pan, Y., Ren, Y., Yao, L., Li, X. "Optimizing solar photovoltaic plant siting in Liangshan Prefecture, China: A policy-integrated, multi-criteria spatial planning framework", Solar Energy, 283, 113012, 2024. https://doi.org/10.1016/j.solener.2024.113012

[33] Sunte, J. "The Design of 1 MW Solar Power Plant", International Journal of Scientific Research in Mechanical and Materials Engineering, 6(4), pp. 27–35, 2022. [online] Available at: https://ijsrmme.com/paper/IJSRMME22644.pdf [Accessed: 14 July 2025]

[34] Zidane, T. E. K., Aziz, A. S., Zahraoui, Y., Kotb, H., AboRas, K. M., Kitmo, Jember, Y. B. "Grid-Connected Solar PV Power Plants Optimization: A Review", IEEE Access, 11, pp. 79588–79608, 2023. https://doi.org/10.1109/ACCESS.2023.3299815

[35] Kolahi, M., Esmailifar, S. M., Moradi Sizkouhi, A. M., Aghaei, M. "Digital-PV: A digital twin-based platform for autonomous aerial monitoring of large-scale photovoltaic power plants", Energy Conversion and Management, 321, 118963, 2024. https://doi.org/10.1016/j.enconman.2024.118963

[36] Bhau, G. V., Deshmukh, R. G., Kumar, T. R., Chowdhury, S., Sesharao, Y., Abilmazhinov, Y. "IoT based solar energy monitoring system", Materials Today: Proceedings, 80, pp. 3697–3701, 2023. https://doi.org/10.1016/j.matpr.2021.07.364

[37] Esmaeilion, F., Ahmadi, A., Esmaeilion, A., Ehyaei, M. A. "The Performance Analysis and Monitoring of Grid-connected Photovoltaic Power Plant", Current Chinese Computer Science, 1(1), pp. 77–96, 2021. https://doi.org/10.2174/2665997201999200511083228

[38] Ibrahim, M., Alsheikh, A., Awaysheh, F. M., Alshehri, M. D. "Machine Learning Schemes for Anomaly Detection in Solar Power Plants", Energies, 15(3), 1082, 2022. https://doi.org/10.3390/en15031082

[39] Emamian, M., Eskandari, A., Aghaei, M., Nedaei, A., Sizkouhi, A. M., Milimonfared, J. "Cloud Computing and IoT Based Intelligent Monitoring System for Photovoltaic Plants Using Machine Learning Techniques", Energies, 15(9), 3014, 2022. https://doi.org/10.3390/en15093014

[40] Khasanov, D., Khujamatov, K., Fayzullaev, B., Reypnazarov, E. "WSN-based Monitoring Systems for the Solar Power Stations of the Telecommunication Devices", IIUM Engineering Journal, 22(2), pp. 98–118, 2021. https://doi.org/10.31436/iiumej.v22i2.1464

[41] Ferlito, S., Ippolito, S., Santagata, C., Schiattarella, P., Di Francia, G. "A Study on an IoT-Based SCADA System for Photovoltaic Utility Plants", Electronics, 13(11), 2065, 2024. https://doi.org/10.3390/electronics13112065

[42] Livera, A., Theristis, M., Micheli, L., Fernández, E. F., Stein, J. S., Georghiou, G. E. "Operation and Maintenance Decision Support System for Photovoltaic Systems", IEEE Access, 10, pp. 42481–42496, 2022. https://doi.org/10.1109/ACCESS.2022.3168140

[43] Udo, W. S., Kwakye, J. M., Ekechukwu, D. E., Ogundipe, O. B. "Predictive Analytics for Enhancing Solar Energy Forecasting and Grid Integration", Engineering Science & Technology Journal, 4(6), pp. 589–602, 2023. https://doi.org/10.51594/estj.v4i6.1394

[44] Schmela, M., Rossi, R., Lits, C., Chunduri, S. K., Shah, A., …, Saratchandra, P. "Advancements in solar technology, markets, and investments – A summary of the 2022 ISA World Solar Reports", Solar Compass, 6, 100045, 2023. https://doi.org/10.1016/j.solcom.2023.100045

[45] Edmunds, C., Galloway, S., Elders, I., Bukhsh, W., Telford, R. "Design of a DSO-TSO balancing market coordination scheme for decentralised energy", IET Generation, Transmission & Distribution, 14(5), pp. 707–718, 2020. https://doi.org/10.1049/iet-gtd.2019.0865

[46] Pena-Bello, A., Junod, R., Ballif, C., Wyrsch, N. "Balancing DSO interests and PV system economics with alternative tariffs", Energy Policy, 183, 113828, 2023. https://doi.org/10.1016/j.enpol.2023.113828

[47] Pintér, G., Zsiborács, H. "Photovoltaic Energy Generation in Hungary: Potentials of Green Hydrogen Production by PEM Technology: First Steps towards the Deployment of the Power-to-gas Technology", Periodica Polytechnica Mechanical Engineering, 67(4), pp. 340–349, 2023. https://doi.org/10.3311/PPme.23333

[48] Zsiborács, H., Vincze, A., Pintér, G., Baranyai, N. H. "The Accuracy of PV Power Plant Scheduling in Europe: An Overview of ENTSO-E Countries", IEEE Access, 11, pp. 74953–74979, 2023. https://doi.org/10.1109/ACCESS.2023.3297494

[49] Pintér, G., Zsiborács, H., Hegedűsné Baranyai, N., Vincze, A., Bertók, M. "Eljárás aktív napkövető napelemes rendszer vezérlésére, valamint kapcsolási elrendezés az eljárás megvalósítására" (A method for controlling an active solar tracking system and a circuit arrangement for implementing the method), Veszprém, Hungary, P2300095, 2023. (in Hungarian).

[50] Wattler Kft. "Napelemek aFRR-kötelezettsége felfüggesztve" (aFRR obligation for solar PV systems suspended), [online] Available at: https://wattler.eu/2023/01/afrr-felfuggesztes/ [Accessed: 26 October 26 2023] (in Hungarian)

[51] PV Napenergia Kft. "Az aFRR-kötelezettség felfüggesztésének hatása a napelemes beruházásokra" (The impact of the suspension of the aFRR obligation on PV investments), [online] Available at: https://pvnapenergia.hu/az-afrr-kotelezettseg-felfuggesztesenek-hatasa-a-napelemes-beruhazasokra/ [Accessed: 26 October 2023] (in Hungarian)

[52] Kacskovics, N. J. "Változás jöhet a hazai naperőmű szabályozásban" (Changes could come to PV power plant regulation in Hungary), Forbes, 13 January 2025. [online] Available at: https://www.forbes.hu/uzlet/valtozas-johet-a-hazai-naperomu-szabalyozasban/ [Accessed: 15 July 2025] (in Hungarian)

[53] Major, A. "Fontos kötelezettség szűnhet meg sok naperőmű számára" (Important obligation for many PV power plants could be removed), Portfolio, 13 January 2025. [online] Available at: https://www.portfolio.hu/gazdasag/20250113/fontos-kotelezettseg-szunhet-meg-sok-naperomu-szamara-733815# [Accessed: 15 July 2025] (in Hungarian)

[54] Hussain, M. T., Tariq, M., Sarwar, A., Urooj, S., BaQais, A., Hossain, M. A. "Atomic Orbital Search Algorithm for Efficient Maximum Power Point Tracking in Partially Shaded Solar PV Systems", Processes, 11(9), 2776, 2023. https://doi.org/10.3390/pr11092776

[55] Khan, M. S., Ramli, M. A. M., Sindi, H. F., Hidayat, T., Bouchekara, H. R. E. H. "Estimation of Solar Radiation on a PV Panel Surface with an Optimal Tilt Angle Using Electric Charged Particles Optimization", Electronics, 11(13), 2056, 2022. https://doi.org/10.3390/electronics11132056

[56] Saint-Drenan, Y.-M., Wald, L., Ranchin, T., Dubus, L., Troccoli, A. "An approach for the estimation of the aggregated photovoltaic power generated in several European countries from meteorological data", Advances in Science and Research, 15, pp. 51–62, 2018. https://doi.org/10.5194/asr-15-51-2018

[57] Jamroen, C., Komkum, P., Kohsri, S., Himananto, W., Panupintu, S., Unkat, S. "A low-cost dual-axis solar tracking system based on digital logic design: Design and implementation", Sustainable Energy Technologies and Assessments, 37, 100618, 2020. https://doi.org/10.1016/j.seta.2019.100618

[58] Ngo, X. C., Nguyen, T. H., Do, N. Y., Nguyen, D. M., Vo, D.-V. N., …, Le, Q. V. "Grid-Connected Photovoltaic Systems with Single-Axis Sun Tracker: Case Study for Central Vietnam", Energies, 13(6), 1457, 2020. https://doi.org/10.3390/en13061457

[59] Sun, L., Bai, J. "A device for enhancing the irradiance of bifacial photovoltaic modules and its tracking algorithm", Solar Energy, 298, 113731, 2025. https://doi.org/10.1016/j.solener.2025.113731

[60] Precedence Research "Solar Tracker Market Size, Share and Trends 2025 to 2034", [online] Available at: https://www.precedenceresearch.com/solar-tracker-market [Accessed: 30 July 2025]

[61] Khalil, F. A., Asif, M., Anwar, S., ul Haq, S., Illahi, F. "Solar Tracking Techniques and Implementation in Photovoltaic Power Plants: a Review", Proceedings of the Pakistan Academy of Sciences: A. Physical and Computational Sciences, 54(3), pp. 231–241, 2017. [online] Available at: https://www.paspk.org/wp-content/uploads/2017/09/Solar-Tracking-Techniques.pdf [Accessed: 15 July 2025]

[62] AL-Rousan, N., Isa, N. A. M., Desa, M. K. M. "Advances in solar photovoltaic tracking systems: A review", Renewable and Sustainable Energy Reviews, 82, pp. 2548–2569, 2018. https://doi.org/10.1016/j.rser.2017.09.077

[63] Eke, R., Senturk, A. "Performance comparison of a double-axis sun tracking versus fixed PV system", Solar Energy, 86(9), pp. 2665–2672, 2012. https://doi.org/10.1016/j.solener.2012.06.006

[64] Fuke, P., Yadav, A. K., Anil, I. "Techno-Economic Analysis of Fixed, Single and Dual-Axis Tracking Solar PV System", In: 2020 IEEE 9th IEEE Power India International Conference (PIICON), Sonepat, India, 2020, pp. 1–6. ISBN 978-1-7281-6664-3 https://doi.org/10.1109/PIICON49524.2020.9112891

[65] Hariri, N. G., AlMutawa, M. A., Osman, I. S., AlMadani, I. K., Almahdi, A. M., Ali, S. "Experimental Investigation of Azimuth- and Sensor-Based Control Strategies for a PV Solar Tracking Application", Applied Sciences, 12(9), 4758, 2022. https://doi.org/10.3390/app12094758

[66] Salih, R. A., Mohammed, K. Q., Hama, P. O., Hassan, R. O., Noori, B. K. "Design and Implementation of Single Axis Solar Tracking System: Utilizing GPS, Astronomical Equations, and Satellite Dish Actuator for Optimal Efficiency", Journal of Engineering, 31(2), pp. 95–109, 2025. https://doi.org/10.31026/j.eng.2025.02.06

[67] Harrou, F., Sun, Y., Taghezouit, B., Dairi, A. "Artificial Intelligence Techniques for Solar Irradiance and PV Modeling and Forecasting", Energies, 16(18), 6731, 2023. https://doi.org/10.3390/en16186731

[68] Prinsloo, G. J., Dobson, R. T. (eds.) "Solar Tracking, Sun Tracking, Sun Tracker, Solar Tracker, Follow Sun, Sun Position", SolarBooks, 2015. ISBN 978-0-620-61576-1 https://doi.org/10.13140/2.1.2748.3201

[69] Yang, Z., Xiao, Z. "A Review of the Sustainable Development of Solar Photovoltaic Tracking System Technology", Energies, 16(23), 7768, 2023. https://doi.org/10.3390/en16237768

[70] FUSIONSEEKER "Instruction manuals for FUSIONSEEKER solar tracker controllers", [online] Available at: http://www.fusion-seeker.com/download.html [Accessed: 22 September 2021]

[71] Prinsloo, G. J. "Hardware Sun Tracking Systems and Digital Sun Position Hardware Solar Tracker Controllers", In: Prinsloo, G. J., Dobson, R. T. (eds.) Solar Tracking, Sun Tracking, Sun Tracker, Solar Tracker, Follow Sun, Sun Position, SolarBooks, 2016, pp. 1–35. ISBN 978-0-620-61576-1 https://doi.org/10.13140/RG.2.1.4684.5046

[72] Oosting, K., Inspired Surgical Technologies Inc. "Actuated feed-forward controlled solar tracking system", Scottsdale, AZ, USA, EP2389547A4 (Withdrawn), 2010.

[73] Taylor, R., Evans, C. R., Crain, A., Megawatt Solar Inc. "Methods, systems, and computer readable media for controlling orientation of a photovoltaic collection system to track apparent movement of the sun", Frisco, TX, USA, WO2009048879A3 (Ceased), 2008.

[74] Adest, M., Sella, G., Handelsman, L., Galin, Y., Fishelov, A., SolarEdge Technologies Ltd. "Photovoltaic system power tracking method", Herzlia, IL, USA, US9291696B2 (Active), 2008.

[75] Almy, C., Jensen, S., Tesla Inc. "Oscillation brake for solar tracking system", Austin, TX, USA, US20170187327A1 (Active), 2015.

[76] Williams, C. J., Kliot, G., Lin, C.-C., Harris, S. L., Belady, C. L., Peterson, E. C., Microsoft Technology Licensing LLC. "Localized weather prediction through utilization of cameras", Redmond, WA, USA, US20190072992A1 (Active), 2018.

[77] Drees, K. H., Con Edison Battery Storage LLC. "Photovoltaic energy system with solar intensity prediction", Valhalla, NY, USA, US10554170B2 (Active), 2016.

[78] Nukada, K., Takahata, M., Tamura, T., NTT Docomo Inc. "Control device, program", Tokyo, Japan, JP2014236541A (Active), 2013.

[79] Safaei, F. R. P., Tesla Inc. "Systems and methods for controlling PV production within energy export constraints", Austin, TX, USA, US10139847B2 (Active), 2016.

[80] Michelena, E. G., Razquin, A. P., Echeverria, D. R., Palomo, L. M., Alvarez, J. M., Laita, I. D. L. P., Solano, M. G., Acciona Generacion Renovable SA. "Method for the control of power ramp-rates minimizing energy storage requirements in intermittent power generation plants", Navarra, Spain, EP3026774B1 (Active), 2014.

[81] eBay Inc. "Napelemes nyomkövető kéttengelyes napelemes nyomkövető rendszer napelemes nyomkövető vezérlő" (Solar Tracker Dual Axis Solar Tracking System Solar Tracking Controller), [online] Available at: https://www.ebay.com/itm/316703438444?_skw=dual+axis+tracking&itmmeta=01K0Q8BW4R4Q9G-4JBJS1G6Q10V&hash=item49bcfef66c:g:pjwAAOSwrnBlM-jR0&itmprp=enc%3AAQAKAAAA0FkggFvd1GGDu0w3yX-Cmi1daiOce6V0DCV5Y4AREZbewu0FuNuh4TYRkHe-jpaMDdJKCZPGpYR0lyjyawhth3Mf%2Bjp9hXLLaqOi0uC-6QpzGfvrGZLfSw16AslEB0W44zT9cfi4KS8oAQ4k4HmOfu-CO7s2sM178o7dKH5fOIKo0bGrotqAzmcohSKu%2FGdq42QonTkUVoEe3Fa5FzyktGWSD5yhsp3IgelB6VHVzvxd29VY2DQcNGZvWwkHXJlIE8bwOspCc2fgRRW7RoEnz3VHd7A%3D%7Ctkp%3ABk9SR-LCr-iFZg [Accessed: 26 July 2025] (in Hungarian)

[82] eBay Inc. "Egy/kéttengelyes napelemes nyomkövető vezérlő + relémodul + fényérzékelő SJ" (Single/Dual Axis Solar Tracking Tracker Controller+Relay Module +Light Sensor SJ), [online] Available at: https://www.ebay.com/itm/275467020683?_skw=Dual+Axis+Solar+Tracker&itmmeta=01K0Q8SZXWVMS2C8QJH1BA7RZ5&hash=item40231d298b:g:C44AAOSwY-Jlj7kz&itmprp=enc%3AAQAKAAAA8FkggFvd1GGDu0w3yXCmi1faOdEdYWMS0eS1SqoBpLqCFQyvlji4QCPWHJiaOXxgFpDfMb0NLmT6P8B2mraQsSeZPtyonDJ508KgX61dwJVPWa1TjtGIHp0DROBrOYxeZucLhzYxY6EhEQRctFoh3kApUJkx8DrKCU67gwGvma0lK6lnliLm8xbSsaycYBkQjeEUVQWBvCNpxDrrvPp1INqQq5y%2FOQ%2BsofjdPmN5OPDAGaJ7bhf7J5zk%2Fxth-V7gJ0m9jvSVSozwO%2F8q8GMsOZcZJct5CF9HL-rtqnZvpPLDWffS6jw7gsHKXMc6b0zcGRbw%3D%3D%7Ctkp%3ABFBMmP_n6IVm [Accessed: 22 July 2025] (in Hungarian)

[83] Zsiborács, H., Hegedűsné Baranyai, N., Vincze, A., Háber, I., Weihs, P., Oswald, S., Gützer, C., Pintér, G. "Changes of Photovoltaic Performance as a Function of Positioning Relative to the Focus Points of a Concentrator PV Module: Case Study", Applied Sciences, 9(16), 3392, 2019. https://doi.org/10.3390/app9163392

[84] Fraunhofer Institute for Solar Energy Systems ISE "Photovoltaics Report", Fraunhofer Institute for Solar Energy Systems ISE, Freiburg, Germany, 2025. [online] Available at: https://www.ise.fraunhofer.de [Accessed: 10 December 2025]

[85] Nsengiyumva, W., Chen, S. G., Hu, L., Chen, X. "Recent advancements and challenges in Solar Tracking Systems (STS): A review", Renewable and Sustainable Energy Reviews, 81, pp. 250–279, 2018. https://doi.org/10.1016/j.rser.2017.06.085

[86] Zsiborács, H., Pintér, G., Vincze, A., Hegedűsné Baranyai, N. "A Control Process for Active Solar-Tracking Systems for Photovoltaic Technology and the Circuit Layout Necessary for the Implementation of the Method", Sensors, 22(7), 2564, 2022. https://doi.org/10.3390/s22072564

[87] Python Software Foundation "Python (3.12.5)", [computer program] Available at: https://www.python.org/ [Accessed: 15 September 2025]

[88] HOMER Energy LLC. "HOMER Pro (3.18.4)", [computer program] Available at: https://www.homerenergy.com/products/pro/index.html [Accessed: 03 November 2025]

[89] MicroPython Project. "MicroPython (1.23.0)", [computer program] Available at: https://micropython.org/ [Accessed: 15 September 2025]

Appendix A

Algorithm A1 Simplified pseudocode of the schedule-tracking control loop

Initialization

1. Load schedule M_t, measured actual data P_t, and current tracker position (θ_t, φ_t).
2. Set control interval Δt = 1 min.
3. Set tolerance ε = 3%.
4. Set mechanical deflection limit = ±30°.

Control cycle (for each control step t during the operating period)

5. Read schedule value M_t and actual performance P_t.
6. Compute current solar position (azimuth, elevation).
7. Retrieve actual tracker orientation.
8. Compute deviation $\Delta P_t = P_t - M_t$.
9. If $|\Delta P_t| \leq \varepsilon \times M_t$ then continue default dual-axis tracking and proceed to the next step.
10. Suspend default tracking and perform regulation:
    - 10.1 If $P_t < M_t$ (underproduction), apply corrective deflection toward the optimal position (within ±30°).
    - 10.2 Else (overproduction), detune orientation away from the sun (within ±30°) to limit power output.
11. Recalculate corrected output $P_t^{dual,mech}$.
12. If deviation $\leq \varepsilon \times M_t$ or the mechanical limit is reached, restart normal tracking.
13. Freeze orientation for Δt_{stab} = 1 min and repeat the cycle until the end of the operating period.